JOURNAL OF MATERIALS SCIENCE: MATERIALS IN MEDICINE **16** (2005) 387–392

Influence of ferrous iron incorporation on the structure of hydroxyapatite

R. MORRISSEY, L. M. RODRÍGUEZ-LORENZO, K. A. GROSS*
School of Physics & Materials Engineering, Monash University, VIC 3800, Australia
E-mail: karlis.gross@spme.monash.edu.au

Iron is a vital element of cellular function within the body. High concentrations of iron can be found in the kidneys and the circulatory system. In bones and teeth it is present as a trace element. The use of iron-based compounds in combination with hydroxyapatite offers a new alternative for prosthetic devices. This work investigates the synthesis and processing of iron containing apatites as a possible new type of ceramic for biomedical devices. Stoichiometric and calcium deficient iron containing apatites were synthesized by a wet chemical reaction with di-ammonium-hydrogen-phosphate, calcium nitrate and a ferrous iron nitrate solution. A secondary phase of tri-calcium-phosphate (TCP) was observed after heat treatment of iron containing, calcium deficient, hydroxyapatite. The apatite structure was maintained after heat treatment of stoichiometric apatite, synthesized in the presence of iron. Sintering in air produced oxidation of Fe^{2+} to Fe^{3+}, resulting in the formation of hematite as a secondary phase. The introduction of iron into the synthesis of hydroxyapatite causes: (i) an increase of the a-lattice parameter after synthesis and heat treatment in air; (ii) an increase in the c-lattice parameter after sintering in air.

1. Introduction

Iron is a vital element in the circulatory system and kidneys and is essential for the function of numerous proteins in cells. It is present in the highest oxidation state facilitating oxygen transport and electron transfer, participating in processes for fresh hemoglobin in red blood cells and DNA synthesis in dividing cells. Iron is present at high concentrations in soft organs where it is readily exchanged. The concentration of iron within hard tissue is low, indicating that iron can be present within the body without disturbing the apatite structure and hence the function of bone. Exposure of teeth to externally applied solutions containing iron leads to easier incorporation of iron. This is readily observed by the discolouration of teeth.

Placement of early prosthetic devices manufactured from stainless steels was predominantly aimed at successful integration of these devices into the bone. Incorporation of iron into apatite resident in bone was not of interest and this remains undocumented in the literature. Recent studies have revealed the distribution of iron around an iron based prosthesis [1]. Poor transfer of iron from the circulatory system could infer the low incorporation of dissolved iron from prostheses into hip prostheses.

Iron oxide has been previously incorporated into apatite as a means of increasing the fracture toughness, leading to the possible use as a monolithic implant [2]. These studies were focused on determining the stability of the apatite structure when heated in the presence of iron oxide. Iron may be incorporated into the apatite structure without causing decomposition. The higher temperature can offer a higher driving force for iron incorporation, and little is known about the possible iron accommodating capacity of the apatite structure [3]. The development of iron oxides and iron compounds with apatite would benefit from knowledge of the changes in the lattice and its ability to maintain a single apatite phase. Trends with iron incorporation into the apatite lattice can provide an indication of iron incorporation into the crystal lattice.

This paper reports the preliminary results on the synthesis of Fe^{2+} substituted calcium phosphates apatites. The aim of this work is to determine whether Fe^{2+} is introduced into the apatite structure or remains as a secondary phase when a wet method is employed to synthesize iron-containing apatites. The optimal thermal treatment conditions will be selected with the purpose of controlling the introduction of iron into the apatite structure.

2. Materials and methods

2.1. Materials

Analytical grade $FeCl_2 \cdot 4H_2O$ (99% purity) was obtained from Sigma-Aldrich. Extra purity $(NH_4)_2HPO_4$

*Author to whom all correspondence should be addressed.

and $Ca(NO_3)_2{\cdot}4H_2O$ analytical reagent were both obtained from Riedel-de Haën. All chemicals were used as provided without further purification. High purity nitrogen gas was used during synthesis.

2.2. Synthesis of powders

Apatite powders were synthesized (Refer Table I) by precipitation, based on the HA synthesis chemical reaction,

$$10Ca(NO_3)_2 + 6(NH_4)_2HPO_4 + 8NH_4OH \rightarrow Ca_{10}(PO_4)_6(OH)_2 + 6H_2O + 20NH_4NO_3$$

The first reaction, sample 1, (Refer Table I) contained no ferrous chloride. In this reaction di-ammonium-hydrogen-phosphate was added in 10 mL aliquots from an auto burette, 700 Dosino (Metrohm, Switzerland) into a 1 M calcium nitrate solution. This solution was contained in a closed polypropylene vessel and held at 37 °C for the duration of the reaction. The mixture was buffered to a pH of 9.2 during the reaction by addition of 3.3 vol% ammonia solution with use of a pH stat (736 GP Titrino, Metrohm, Switzerland). The entire reaction was carried out over a period of 8 h under a N_2 atmosphere. The precipitate was matured for 24 h before washing in 2 litres of deionized water, filtering with a Buchner funnel and then washing in 1 litre of ethanol. Powders were dried in an oven purged with nitrogen at 100 °C degrees for 2 days.

Apatite powders containing Fe^{2+} (refer Table I) were synthesized by the same method as for the first reaction, however this time 0.1 M $FeCl_2{\cdot}4H_2O$ was added to the 1 M $Ca(NO_3)_2{\cdot}4H_2O$ solution. In sample 2, iron was added to allow replacement of the calcium in the apatite $Ca_{10}(PO_4)_6(OH)_2$. In sample 3, iron chloride hydrate was added in excess to determine whether the apatite stoichiometry influences iron incorporation. In sample 4, 0.9 M $Ca(NO_3)_2{\cdot}4H_2O$ was used to generate a calcium deficient sample and was produced as a reference for sample 3.

Synthesized powder was calcined at 900 °C. Samples were heated at a constant rate of 10 °C/min and held for 2 h before cooled to room temperature in the furnace. Then powders were sintered at a temperature of 1150 °C in an air and nitrogen atmosphere. Sintered samples were heated at a rate of 2 °C/min.

2.3. Analysis and characterization

Thermal gravimetric analysis (TGA) was carried out in a Setaram TG92. Samples were heated at a constant rate of 2 °C/min up to 1200 °C. The specific surface area of the synthesized powders was determined using a Micromeritics Gemini 2360 (Norcross GA, USA) BET. Each sample tube was de-gassed overnight with nitrogen at 100 °C, to remove physically absorbed water.

Fourier transform infra-red spectroscopy (FTIR) was carried out in a Perkin-Elmer 1600 series FTIR in the 400–4000 cm^{-1} region. KBr pellets were prepared for this analysis under a vacuum and an applied pressure using 1mg of sample and 250 mg of KBr.

X-ray diffraction was performed on synthesized, calcined and sintered powders within a 2θ range of 10–90 degrees using a Rigaku Geigerflex diffractometer with Bragg-Bentano geometry in a step mode with a step size of 0.02° and 10 s per step using Copper K_α radiation at 40 kV and 22.5 mA passing through a 0.5° divergence slit and 0.3° receiver slit. The patterns were used for the purpose of determining lattice parameters.

TABLE I Summary of synthesis schedule

Sample	Code	Iron type	Specific surface area (m^2/g)
1	HA	No Fe present	50
2	HAd-Fe^{2+}	Fe^{2+}	55
3	HA-Fe^{2+}	Fe^{2+}	83
4	HAd	No Fe present	49

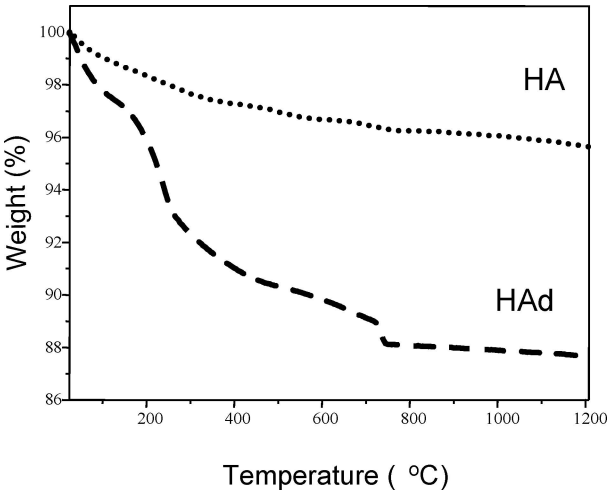

Figure 1 Weight loss curves of a calcium deficient and a stoichiometric apatite sample.

3. Results and discussion

Fig. 1 shows the weight loss curves of a calcium deficient and a stoichiometric apatite. Both samples show weight loss up to 400 °C that can be attributed to by-products such as NO_3^-, ammonia and water, all of which become volatile upon heating. These by-products are assumed to be adsorbed on the surface, as no evidence can be found in the literature indicating that NO_3^- is incorporated into the apatite structure [4]. Incorporation of ammonia ions is expected to be at a low level due to their large size. In previous apatite synthesis it has been shown that other ions, such as K^+ and Na^+, are expected to be incorporated much more readily [5, 6]. The HAd TGA curve also shows the weight loss step between 600 and 750 °C, characteristic of calcium deficient apatite's. This step results from the condensation of the HPO_4^{2-} groups to yield P_2O_7 that react further to yield Ca_3PO_4 plus the volatile H_2O according to the following reactions [7].

$$2HPO_4^{2-} \rightarrow P_2O_7^{4-} + H_2O$$

$$Ca_2P_2O_7 + Ca_{10}(PO_4)_6(OH)_2 \rightarrow 4Ca_3(PO_4)_2 + H_2O$$

A calcination process was performed at 900 °C on all powders to ensure they were free from the residual impurities.

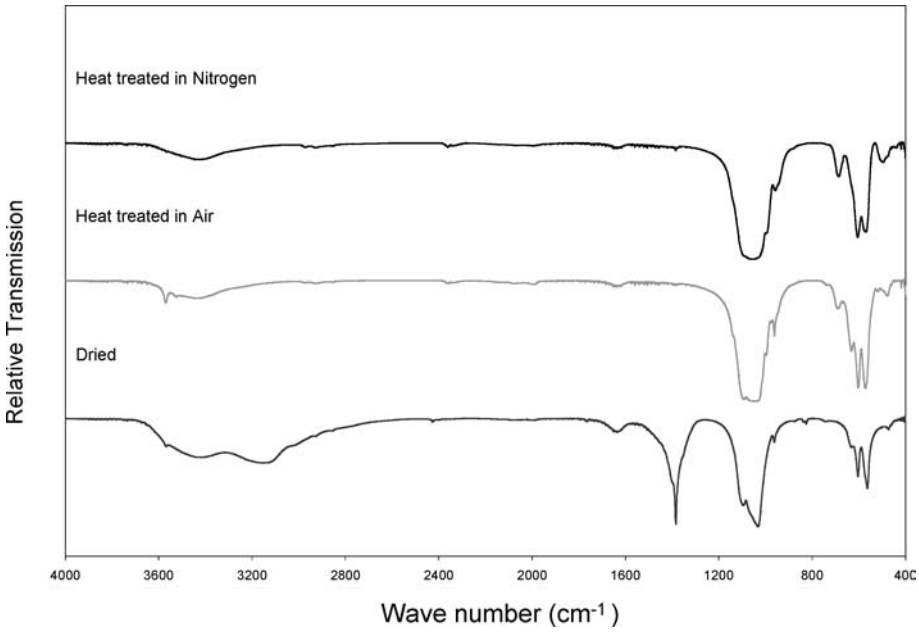

Figure 2 FTIR spectra of HAd- Fe^{2+} in a dried form and after sintering in air and nitrogen.

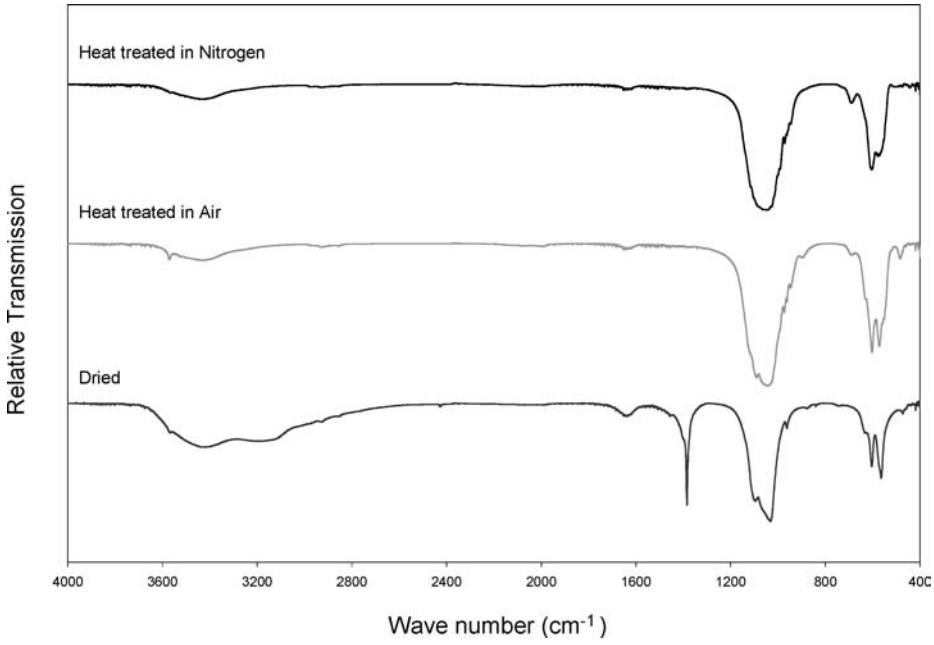

Figure 3 FTIR spectra of HA- Fe^{2+} in a dried form and after sintering in air and nitrogen.

The FTIR spectra of the dried and calcined powders are displayed in Figs. 2–4. Dried powder spectra show vibrational bands characteristic of calcium hydroxyapatite. The band present at 1380 cm^{-1}can be assigned to nitrate and phosphate residual impurities [8]. The group PO_4can be attributed to the strong doublet between 1000 and 1100 cm^{-1} (mode υ_3), the band at 960 cm^{-1} (mode υ_1) and the bands at 605 and 575 cm^{-1} (mode υ_4). The shoulders at 3570 and 630 cm^{-1} can be assigned to an OH^- group in a hydroxyapatite environment and the broad band centered at 3500 cm^{-1} shows the presence of water in the samples [9].

Figs. 4 and 5 show the XRD patterns for the synthesized samples. In the dried state, only a poorly crystalline phase can be seen; there are no peaks that can be assigned to crystalline phases other than apatite. All unmarked peaks in the XRD scans are considered to belong to HA, according to the International Centre for Diffraction Database (ICDD) file no 24-33.

IR spectra of the dried and calcined samples are displayed in Figs. 2–4. The bands attributed to impurities in the dried materials have disappeared and the spectra only shows bands that can be assigned to calcium phosphate compounds. HAd spectra displayed in Fig. 2 exhibit shoulders on the strong band at 1000–1100 cm^{-1}, attributed to a tri-calcium-phosphate (TCP) [10]. The only difference between the spectrum of the powder treated in an air atmosphere and the spectrum of the sample treated in a nitrogen atmosphere is that the former atmosphere leads to peaks at 630 and 3572 cm^{-1}, attributed to hydroxyl groups, not shown in the sample heated in nitrogen. HAd-Fe^{2+} and HA-Fe^{2+} spectra of

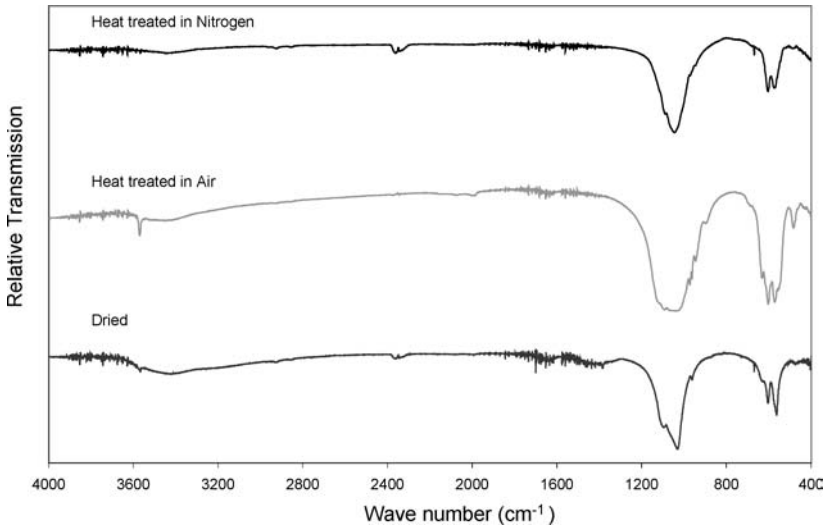

Figure 4 FTIR spectra of HAd in a dried form and after sintering in air and nitrogen.

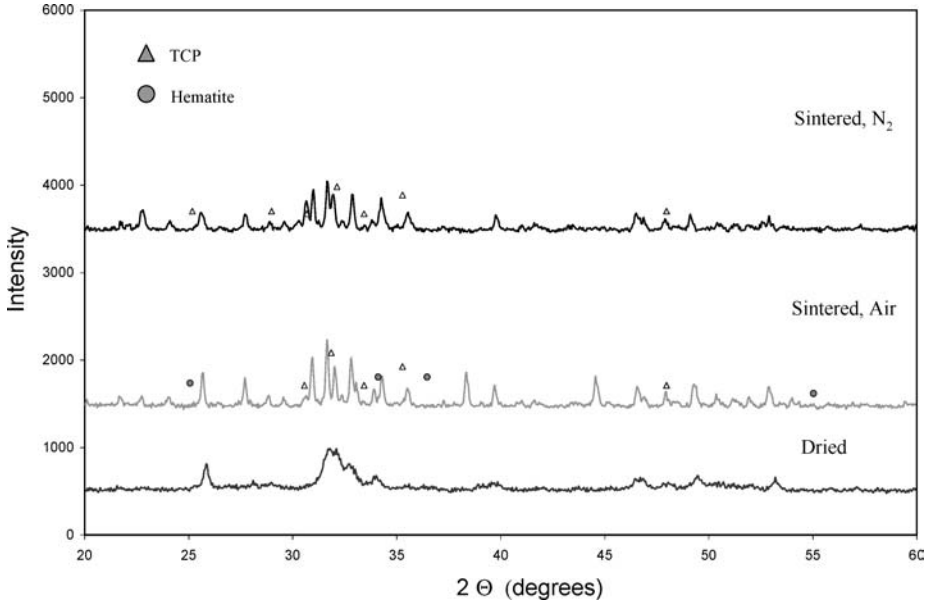

Figure 5 XRD pattern of HAd-Fe^{2+} in a dried form and after sintering in air and nitrogen.

heat-treated powder are analogous to the formerly described sample but have a band at 675 cm^{-1} can also be observed irrespective of the atmosphere used for the treatment.

Figs. 5 and 6 display the XRD patterns of the heat-treated powders. A secondary phase of TCP can be observed when HAd-Fe^{2+} is heat treated in both atmospheres. The lack of TCP in the HA-Fe^{2+} sample can be attributed to the correct stoichiometric ratio of Ca: P that is present during the synthesis. This result correlates with the findings of the FTIR spectra whereby a band characteristic of TCP can be seen for the HAd-Fe^{2+} sample and not for the HA-Fe^{2+} sample.

The XRD scans of HA-Fe^{2+} and HAd-Fe^{2+} also exhibit a shift in the position of the peaks, when the samples are heat treated in the two different atmospheres. This can be easily observed for the three highest peaks within the range 30–35°. The most dramatic peak shift can be seen when they are heat treated in nitrogen. This peak shift may correlate to a change in lattice parameters. XRD patterns of heat treated samples also show the presence of Hematite, Fe_2O_3, (diffraction card 33-664 [22]) in HA-Fe^{2+} and HAd-Fe^{2+} when heat-treated in air and the lack of this phase when heat-treated in nitrogen. This observation indicates that the iron oxidation has been prevented when a nitrogen atmosphere has been used but to check whether Fe^{2+} is moving into the HA structure.

The specific surface area results are shown in Table I. The inverse relationship between surface area and particle size suggests that the presence of ferrous iron may inhibit the growth of precipitate particles in comparison to the reference powders of HA & HAd. This is in agreement with other studies that found a decrease in crystallite size when iron was present during the synthesis of stoichiometric hydroxyapatite [11]. The larger surface area suggests that the iron may inhibit crystal growth or produce a secondary iron rich phase with a smaller size precipitate crystal size. Hydroxyapatite sinters at a moderate temperature, 1100–1300 °C [2, 12, 13] so it does not seem necessary to have a very high driving force for the sintering of the ceramic

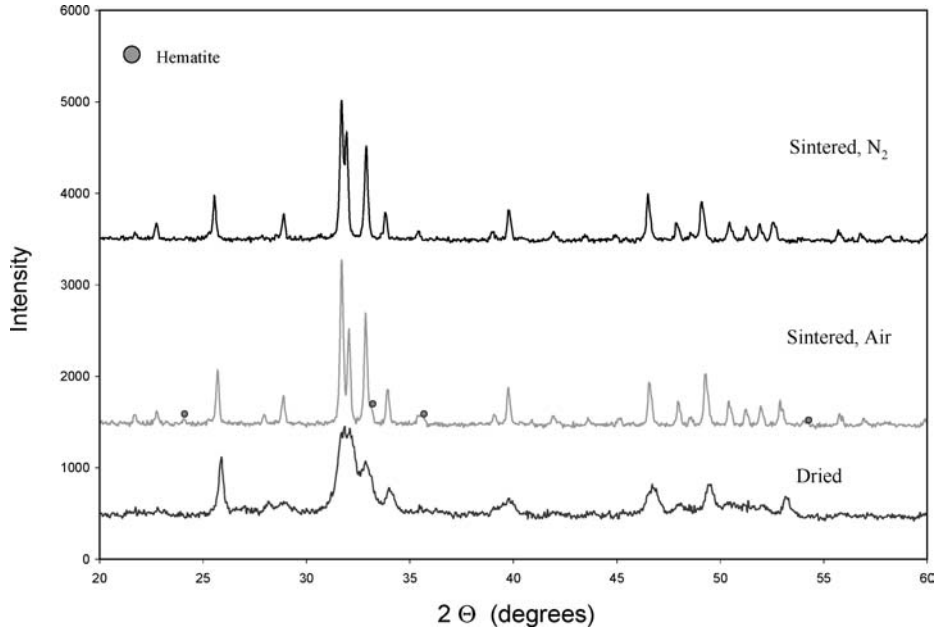

Figure 6 XRD pattern of HA-Fe^{2+} in a dried form and after sintering in air and nitrogen.

bodies. A surface area of 10 m^2/g is suitable for sintering to avoid undesirable agglomerates that can be formed when particles with higher surface area are chosen [14]. Therefore, a thermal treatment of 900 °C that leads to a surface area of about 10 m^2/g was selected for the calcining step and a treatment at 1150 °C was selected for the sintering step. At this temperature, no decomposition of the apatite phases should be expected while obtaining densified bodies.

Analysis of the XRD patterns of all powders suggests that iron is modifying the apatite structure. This is observed in the change to the lattice parameters. These results are provided in Table II. An increase in the a-axis parameter for both HA-Fe^{2+} and HAd-Fe^{2+} and a slight decrease for the HAd sample can be observed on dried and sintered samples when HA is used as a reference. Precipitated apatites generally have an a-lattice parameter from 0.01 to 0.02 Å greater than high temperatures apatites [8], therefore, the lower a-lattice parameter observed for HAd can be expected and the increase in the a-lattice parameter has to be attributed to the iron effect. A greater increase has been obtained when the samples were sintered in a nitrogen atmosphere.

The c-axis was found to increase for iron containing samples in all conditions. The change is greater for samples sintered in air than samples sintered in nitrogen atmosphere. These changes produce changes in the cell volume that can be observed in Fig. 7. Cell volume is greater for HA-Fe^{2+} when sintered in air but is greater for Had-Fe^{2+} when sintered in nitrogen.

Location of iron within the HA structure is dictated by the oxidation state [15]. Iron may exhibit a different

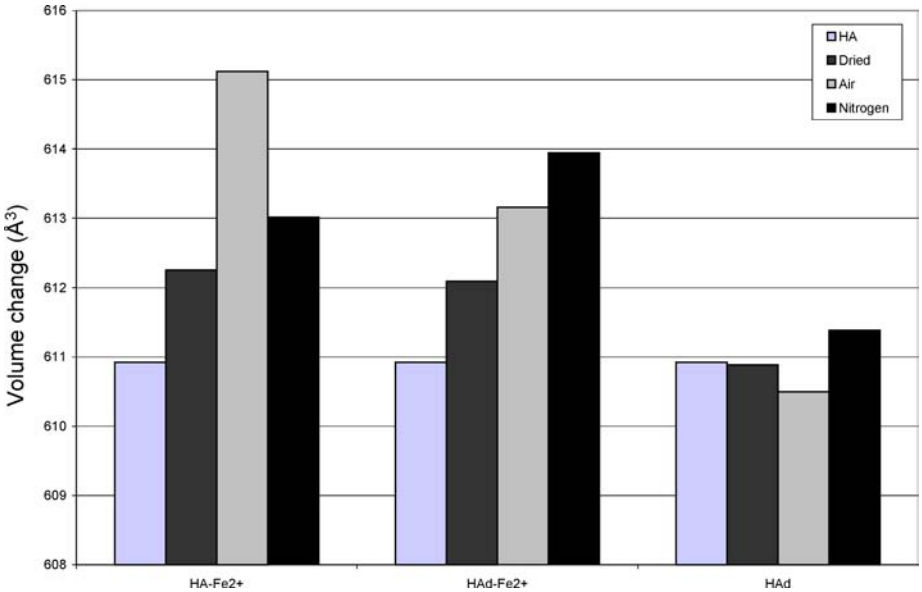

Figure 7 Apatite lattice volume change.

TABLE II Summary of lattice parameters (measurements in Angstroms)

	a			*c*		
Powder	Dried	Sintered, Air	Sintered, N_2	Dried	Sintered, Air	Sintered, N_2
HA	9.4239	–	–	6.8790	–	–
HAd-Fe^{2+}	9.4288	9.4267	9.4410	6.8850	6.9001	6.8880
HA-Fe^{2+}	9.4287	9.4350	9.4358	6.8870	6.9100	6.8852
HAd	9.4230	9.4148	9.3881	6.8799	6.8875	6.9368

degree of occupancy in the Ca_i site as opposed to the Ca_{ii} position within the unit cell. It is not clear whether the two atmospheres used for sintering the samples has produced any change in the oxidation state of the reactant iron involved. Mössbauer spectroscopy may help to solve this question.

4. Conclusions

It is possible to synthesize Fe^{2+} containing apatites using a wet chemistry method. If a single calcium phosphate phase is to be obtained, the synthesis needs to be conducted in the condition that leads to stoichiometric apatite with an additional iron reactant. Sintering in air produced the oxidation of Fe^{2+} to Fe^{3+} that results in a hematite secondary phase. The introduction of iron results in a variation of the hydroxyapatite lattice parameters.

References

1. A. EKTESSABI, *et al.*, *X-ray Spectrom.* **30**(1) (2001) 44.
2. W. SUCHANEK and M. YOSHIMURA, *J. Mater. Res.* **13**(1) (1998) 94.
3. K. A. GROSS, *et al.*, *Europ. Cells and Mater.* **3**(2) (2002) 114.
4. J. L. MEYER and B. O. FOWLER, *Inorg. Chem.* **21** (1982) 3029.
5. S. E. P. DOWKER and J. C. ELLIOTT, *Calcif. Tiss Int.* **29** (1979) 177.
6. *Idem.*, *J. Solid State Chem.* **49** (1983) 334.
7. M. VALLET-REGI, L. M. RODRIGUEZ-LORENZO and A. J. SALINAS, *Solid State Ionics* **101** (1997) 1279.
8. J. C. ELLIOTT, "Structure and Chemistry of the Apatites and Other Calcium Orthophosphates" (Studies in Organic Chemistry, Elsevier, Amsterdam 1994) vol. 18, p. 389.
9. B. O. FOWLER, *Inorg. Chem.* **13**(1) (1974) 194.
10. B. O. FOWLER, E. C. MORENO and W. E. BROWN, *Arch. Oral. Biol.* **11** (1966) 477.
11. B. SUTTER, *et al.*, *Soil. Sci. Soc. Amer. J.* **67**(6) (2003) 1935.
12. J. ZHOU, *et al.*, *J. Mater. Sci.: Mater. Med.* **4** (1993) 83.
13. S. PUAJINDANERT, S. BEST and W. BONDFIELD, *British. Ceram. Trans.* **3** (1993) 96.
14. L. M. RODRIGUEZ-LORENZO, M. VALLET-REGI and J. M. F. FERREIRA, Fabrication of Hydroxyapatite Bodies by Uniaxial Pressing from a Precipitated Powder. *Biomaterials*, 2002.
15. M. JIANG, *et al.*, *Phys. Rev. B* **6622**(22) (2002) 4107.

Received 1 July
and accepted 1 November 2004